

# Metabolic Labeling and Imaging of N-Linked Glycans in *Arabidopsis thaliana*

Yuntao Zhu, Jie Wu, and Xing Chen\*

**Abstract:** Molecular imaging of glycans has been actively pursued in animal systems for the past decades. However, visualization of plant glycans remains underdeveloped, despite that glycosylation is essential for the life cycle of plants. Metabolic glycan labeling in *Arabidopsis thaliana* by using *N*-azidoacetylglucosamine (GlcNAz) as the chemical reporter is reported. GlcNAz is metabolized through the salvage pathway of *N*-acetylglucosamine (GlcNAc) and incorporated into *N*-linked glycans, and possibly intracellular *O*-GlcNAc. Click-labeling with fluorescent probes enables visualization of newly synthesized *N*-linked glycans. *N*-glycosylation in the root tissue was discovered to possess distinct distribution patterns in different developmental zones, suggesting that *N*-glycosylation is regulated in a developmental stage-dependent manner. This work shows the utility of metabolic glycan labeling in elucidating the function of *N*-linked glycosylation in plants.

**P**lants synthesize diverse glycans that are essential for their life cycles. The cell wall, an extracellular matrix surrounding plant cells, is mostly composed of high-molecular-weight polysaccharides, including cellulose, hemicellulose, and pectin.<sup>[1,2]</sup> Furthermore, glycoproteins modified with *N*- or *O*-linked glycans are synthesized in plants and play important functional roles.<sup>[3–5]</sup> Comparing to glycans in animals, plant glycosylation has received relatively less attention for the past several decades.<sup>[6]</sup> As a result, development of techniques for visualizing glycans has mainly focused on animal glycosylation.<sup>[7–9]</sup> In particular, a chemical reporter strategy based on metabolic labeling of glycans with unnatural monosaccharide analogues containing a bioorthogonal functional group (for example, an azide or alkyne) has emerged as a powerful method for glycan imaging and functional studies in animal systems.<sup>[10–12]</sup> The promise of generating renewable energy from glycan-enriched biomass has lately sparked a growing interest in plant glycobiology.<sup>[13]</sup>

The glycan labeling and imaging techniques developed in animal systems, if can be adapted for plants, will be invaluable for probing biosynthesis and biological function of plant glycans.

The glycan biosynthetic pathways in plants possess many distinct features, and a variety of unique plant glycans have been identified.<sup>[6]</sup> Therefore, evaluation of unnatural sugar reporters in plants is critical for developing metabolic glycan labeling methods for plants. For example, 6-alkynyl fucose (FucAl), a fucose analogue containing an alkyne, was used to metabolically label the fucose-containing pectin in cell walls, and no incorporation of FucAl into fucosylated proteins was observed.<sup>[14]</sup> Distinctly, FucAl primarily labels fucosylated proteins in mammalian cells.<sup>[15]</sup> Moreover, an azido analogue of 3-deoxy-D-manno-oct-2-ulosonic acid (Kdo), a monosaccharide that does not exist in animals, was recently exploited to metabolically label pectin.<sup>[16]</sup> Metabolic incorporation of FucAl and azido Kdo into pectins has enabled click-labeling and fluorescence imaging of cell walls.<sup>[14,16]</sup> However, metabolic labeling of plant protein glycans has not been reported. Herein, we report the development of a strategy for metabolic labeling and imaging of protein *N*-glycans in *Arabidopsis thaliana* (Figure 1).

*N*-linked glycosylation, the attachment of *N*-glycans to asparagine residues within the *N*-!P-S/T (where !P is not proline) consensus sequence of cell surface and secreted proteins, is one of the most prominent protein posttranslational modifications, which occurs in all eukaryotes.<sup>[4,17]</sup> Plant *N*-linked glycosylation has been implicated in protein quality control, development, innate immunity, and stress response.<sup>[5,18–20]</sup> With a conserved pentasaccharide core structure consisting of two *N*-acetylglucosamine (GlcNAc) and three mannose residues, *N*-glycans are classified into three types: high mannose, complex, and hybrid. Built on the core structure, unique glycosidic linkages have been found in plants, such as  $\alpha$ 1,3 fucose to the asparagine-linked GlcNAc and  $\beta$ 1,2 xylose to mannose.<sup>[6]</sup> We were interested in targeting the core structure with *N*-azidoacetylglucosamine (GlcNAz) for metabolic labeling and fluorescent imaging of *Arabidopsis* *N*-glycans (Figure 1 a).

Although metabolic incorporation of GlcNAz into cell-surface *N*-glycans has been demonstrated in mammalian cells, imaging of *N*-glycans is complicated by simultaneous labeling of mucin-type *O*-linked glycans.<sup>[21–26]</sup> With a characteristic  $\alpha$ -linked *N*-acetylgalactosamine (GalNAc) attached to Ser/Thr of cell-surface proteins, mucin-type *O*-glycans contain GlcNAc on the branches. Moreover, metabolic crosstalk between the salvage pathways of GlcNAc and GalNAc enables interconversion between the donor sugar nucleotides, uridine-diphosphate-GlcNAc (UDP-GlcNAc) and UDP-

[\*] Y. Zhu, Prof. X. Chen

College of Chemistry and Molecular Engineering  
Peking University, Beijing, 100871 (China)  
E-mail: xingchen@pku.edu.cn

J. Wu, Prof. X. Chen

Peking-Tsinghua Center for Life Sciences  
Peking University, Beijing, 100871 (China)

Prof. X. Chen

Synthetic and Functional Biomolecules Center, and  
Key Laboratory of Bioorganic Chemistry and Molecular Engineering  
of Ministry of Education  
Peking University, Beijing, 100871 (China)

Supporting information and the ORCID identification number(s) for the author(s) of this article can be found under  
<http://dx.doi.org/10.1002/anie.201603032>.

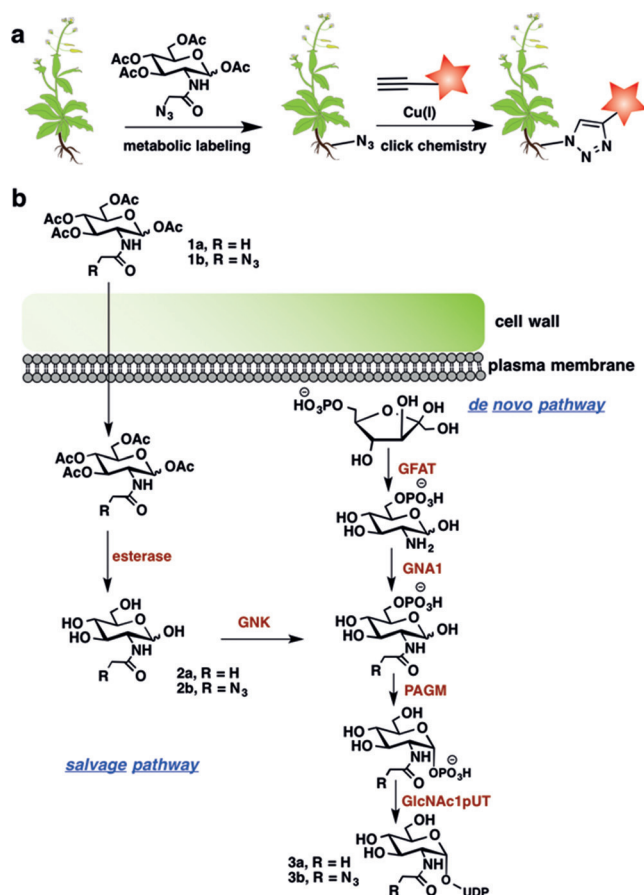


**Figure 1.** Metabolic labeling of *Arabidopsis* N-linked glycans with  $\text{Ac}_4\text{GlcNAz}$ . a)  $\text{Ac}_4\text{GlcNAz}$  is fed to *Arabidopsis* seedlings grown in liquid medium and incorporated into N-linked glycans through the GlcNAc salvage pathway. The GlcNAz-incorporated seedlings are reacted with an alkyne-containing probe via click chemistry. b)  $\text{Ac}_4\text{GlcNAz}$  (**1b**) diffuses through the cell wall and membrane, and is hydrolyzed by cytosolic esterases. The resulting GlcNAz (**2b**) enters the salvage pathway and is eventually converted into UDP-GlcNAz (**3b**), a nucleotide sugar donor for N-linked glycosylation. In the de novo biosynthetic pathway, GlcNAz is synthesized from fructose-6-phosphate, and then converted into UDP-GlcNAc. GFAT, glutamine:fructose-6-phosphate amidotransferase; GNA1, GlcN-6-phosphate acetyltransferase; PAGM, phosphoacetylglucosamine mutase; GlcNAc1-pUT, GlcNAc-1-phosphate uridylyltransferase; GNK, GlcNAc kinase.

GalNAc, as well as their azido analogues.<sup>[23]</sup> As a result, azido or alkynyl analogues of GlcNAc or GalNAc may label multiple glycans with varied specificity. For instance, metabolic labeling of mammalian cells with peracetylated *N*-azidoacetylglactosamine ( $\text{Ac}_4\text{GalNAz}$ ) results in azide-incorporation into N-glycans, mucin-type O-glycans, and O-GlcNAc.<sup>[26]</sup> O-GlcNAylation, attachment of a single GlcNAc monosaccharide to Ser/Thr of various intracellular proteins, occurs in various eukaryotes.<sup>[27]</sup>

In *Arabidopsis*, mucin-type O-linked glycosylation does not occur and no other GalNAc-containing glycan has been found.<sup>[28,29]</sup> Notably, O-GlcNAc modification of intracellular proteins has been identified in *Arabidopsis*.<sup>[30–32]</sup> Even if  $\text{Ac}_4\text{GalNAz}$  could be metabolically incorporated into both N-glycans and O-GlcNAc, they would be easily distinguished by

their distinct subcellular locations, for the purpose of click-labeling and fluorescent imaging. In the de novo GlcNAc biosynthetic pathway of *Arabidopsis*, UDP-GlcNAc is produced from fructose-6-phosphate via a series of enzymatic steps (Figure 1b). All of the intermediates in this pathway are phosphorylated compounds; using analogues of those compounds as chemical reporters is practically cumbersome because the negative charge hinders cellular uptake and synthesizing phosphorylated derivatives is chemically challenging. It was not until recently that the existence of a GlcNAc salvage pathway in plants became evident. An *lignescens* (*lig*) mutant of *Arabidopsis*, which bears a mutation in glucosamine-6-phosphate acetyltransferase (GNA), was isolated and exhibited temperature-dependent growth defects due to the impaired UDP-GlcNAc biosynthesis.<sup>[33]</sup> The growth defects could be suppressed by adding exogenous GlcNAc. The presence of a GlcNAc salvage pathway in *Arabidopsis* was further supported by identification of *Arabidopsis* GlcNAc kinase (GNK), an essential enzyme for the salvage of GlcNAc.<sup>[34]</sup> Therefore, we reasoned that the GlcNAc salvage pathway in *Arabidopsis* might be exploited to convey GlcNAz into the N-linked glycans (Figure 1b).

GlcNAz was chemically synthesized and globally acetylated as  $\text{Ac}_4\text{GlcNAz}$  to facilitate the cellular uptake.<sup>[22]</sup> *Arabidopsis* Col-0 seedlings were incubated with  $100\ \mu\text{M}$   $\text{Ac}_4\text{GlcNAz}$  in liquid Murashige and Skoog (MS) mineral medium for 48 h (Figure 1a). The GlcNAz-incorporated seedlings were fixed with 4% paraformaldehyde, followed by reacting with alkyne–Alexa Fluor 488 via Cu<sup>I</sup>-catalyzed azide–alkyne cycloaddition (CuAAC, also termed click chemistry). Fluorescence microscopy on the labeled seedlings showed significant fluorescence in the root tissue (Figure 2a,b). In contrast, seedlings incubated with the DMSO vehicle or seedlings that were fixed with PFA before  $\text{Ac}_4\text{GlcNAz}$ -treatment exhibited only background fluorescence, suggesting that GlcNAz is metabolically incorporated into cellular glycans in the living plants. Since the alkyne–Alexa Fluor 488 dye is membrane-impermeable, only the cell-surface and extracellular glycans with azides might be fluorescently labeled. Confocal fluorescence imaging revealed that the GlcNAz-dependent fluorescence was mainly distributed on the surfaces of root epidermal cells, which is in agreement with the localization of the N-linked glycoproteins (Figure 2c). Metabolic incorporation of GlcNAz into N-linked glycans is dose- and time-dependent. The discernible fluorescence labeling was achieved at  $\text{Ac}_4\text{GlcNAz}$  concentrations above  $10\ \mu\text{M}$  (Figure 2d; Supporting Information, Figure S1). The GlcNAz-dependent fluorescence increased over time from 24 h to 72 h (Figure 2e; Supporting Information, Figure S2). Furthermore, incubation with  $200\ \mu\text{M}$   $\text{Ac}_4\text{GlcNAz}$  for up to 120 h caused no significant toxic effect on the seedling growth, as shown by the root-length assay (Supporting Information, Figure S3).

To assay whether  $\text{Ac}_4\text{GlcNAz}$  was metabolized through the GlcNAc salvage pathway as depicted in Figure 1b, we treated the seedlings with  $\text{Ac}_4\text{GlcNAz}$  in the presence of excess  $\text{Ac}_4\text{GlcNAc}$  (Figure 3a,b). Cell-surface fluorescence was competitively suppressed, indicating that  $\text{Ac}_4\text{GlcNAz}$  is taken up by the seedlings, hydrolyzed by intracellular

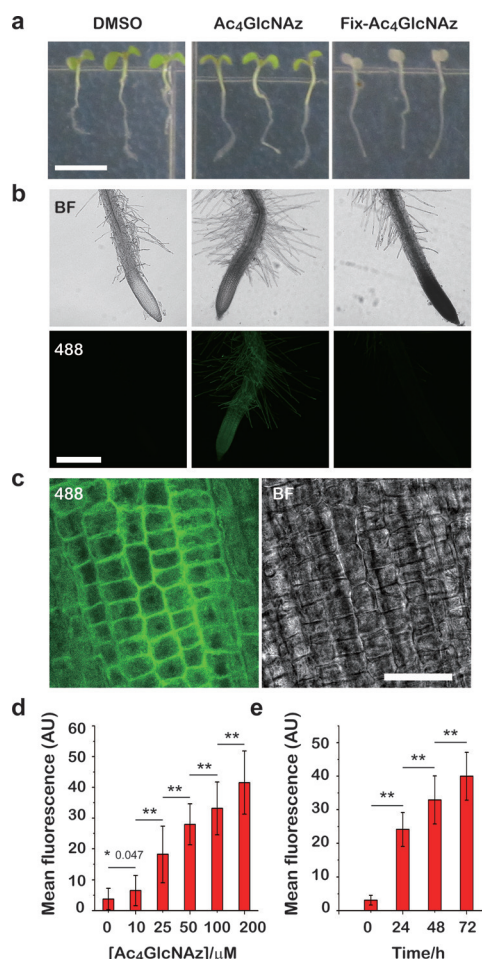


**Figure 2.** Click-labeling and fluorescence imaging of Ac<sub>4</sub>GlcNAz-treated *Arabidopsis* seedlings. a) Representative pictures of 4-day-old *Arabidopsis* seedlings incubated with DMSO or 100 μM Ac<sub>4</sub>GlcNAz for 48 h, followed by fixation with 4% PFA for 30 min. The right panel shows seedlings that were fixed by PFA before treating with 100 μM Ac<sub>4</sub>GlcNAz for 48 h. Scale bar: 5 mm. b) Bright-field and fluorescence images of the root tissue. The seedlings were treated as described in (a), followed by reaction with 1 μM alkyne–Alexa Fluor 488 via CuAAC. The images were collected with a 10× objective lens on a confocal microscope. Scale bar: 400 μm. c) Confocal fluorescence and bright-field images of root epidermal cells in seedlings treated with Ac<sub>4</sub>GlcNAz and click-labeled with alkyne–Alexa Fluor 488. The images were collected with a 63× oil-immersion objective lens on a confocal microscope. Scale bar: 50 μm. d), e) The dose- and time-dependence of GlcNAz incorporation. Seedlings were treated with Ac<sub>4</sub>GlcNAz at varying concentrations for 48 h (d) or with 100 μM Ac<sub>4</sub>GlcNAz for varying durations of time (e), followed by reaction with alkyne–Alexa Fluor 488 and confocal fluorescence imaging. The error bars represent the S.D. from more than 60 cells. Data of those cells were collected from six seedlings from three replicate experiments. \*\**P* < 0.01 (one-way ANOVA).

esterases, and converted into UDP-GlcNAz through the GlcNAc salvage pathway. Moreover, we treated the seedlings with tunicamycin, an inhibitor of N-linked glycosylation. Significant reduction of the GlcNAz-dependent fluorescence was observed, indicating that N-glycans were metabolically incorporated with GlcNAz in the Ac<sub>4</sub>GlcNAz-treated seedlings (Figure 3c,d). Metabolic incorporation of azides enables

not only fluorescent imaging, but also enrichment of GlcNAz-incorporated glycoproteins. The Ac<sub>4</sub>GlcNAz-treated seedlings were lysed and reacted with alkyne–biotin via CuAAC, followed by enrichment with streptavidin beads. Western blot analysis showed that a variety of glycoproteins were incorporated with GlcNAz and enriched through click-labeling using the affinity tag (Figure 3e, lane 3). By performing the click reaction in lysates, we may have labeled and enriched both N-linked glycoproteins and O-GlcNAcylated proteins. The enriched glycoproteins were treated on beads with PNGase F, an N-glycan-specific endoglycosidase.<sup>[35]</sup> Of note, complex and hybrid N-glycans with a fucose α1,3-linked to the asparagine-linked GlcNAc are resistant to PNGase F cleavage, and therefore PNGase F treatment in *Arabidopsis* releases proteins glycosylated with N-glycans containing no fucose-modified core structure, such as high mannose type N-glycans. Western blot analysis on the residual proteins on the beads exhibited much less bands, which probably corresponded to proteins with N-glycans containing the α1,3-linked fucose and O-GlcNAcylated proteins incorporated with GlcNAz (Figure 3e, lane 4).

To further establish that N-linked glycosylated proteins were metabolically labeled with GlcNAz, we subjected the PNGase F-released proteins to gel-based proteomic identification by tandem mass spectrometry (Supporting Information, Table S1). A total of 102 proteins were identified, 81 of which were previously reported N-linked glycoproteins.<sup>[4,36,37]</sup> All of the identified proteins contain the consensus sequence of N-linked glycosylation. This pilot proteomic experiment demonstrates that GlcNAz serves as a chemical reporter for N-glycans and may be a powerful tool for studying protein N-linked glycosylation in *Arabidopsis*.

N-linked glycosylation occurs on both the cell wall-embedded proteins and plasma membrane-bound proteins. We sought to visualize the incorporation of GlcNAz into these two types of glycoproteins that are distinct in location. Pontamine Fast Scarlet 4B (S4B), a cellulose-recognizing fluorescent dye,<sup>[38]</sup> was used to stain the cell wall of the seedlings treated with Ac<sub>4</sub>GlcNAz and alkyne–Alexa Fluor 488. Two-color 3D imaging showed that the GlcNAz-dependent labeling not only colocalized with the S4B-stained cell wall but also resided underneath the cell wall, which probably corresponds to the N-glycans on the plasma membrane (Figure 4a). Furthermore, we separated the protoplasm from the cell wall of the labeled seedlings by inducing plasmolysis. In this experiment, FucAl was employed as a marker for the cell wall, since it is mainly incorporated into pectin.<sup>[14]</sup> Seedlings were incubated with Ac<sub>4</sub>GlcNAz and Ac<sub>4</sub>FucAl for 48 h, followed by sequential click-labeling of FucAl and GlcNAz with azide-Cy5 and alkyne–Alexa Fluor 488, respectively. The labeled seedlings were then subjected to plasmolysis in 0.8 M mannitol. GlcNAz-dependent fluorescence was observed both in the cell wall and on the plasma membrane (Figure 4b). Taken together, these data indicate that GlcNAz can be metabolically incorporated into N-linked glycoproteins that locate both in the cell wall and on the cell membrane.

Since GlcNAz is metabolically incorporated, it enables labeling and visualization of newly synthesized N-linked



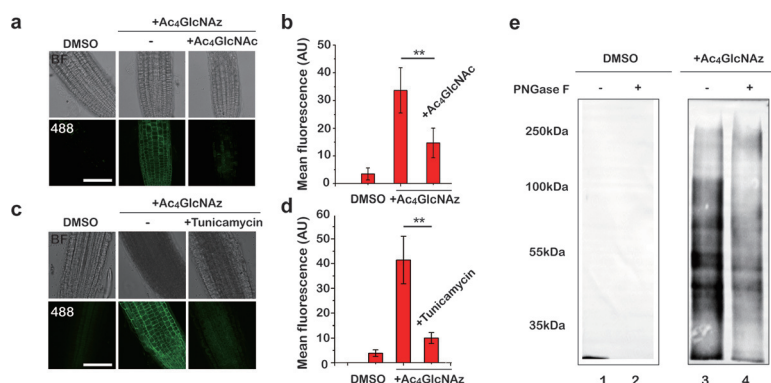


**Figure 3.** Metabolic fate of Ac<sub>4</sub>GlcNAz in *Arabidopsis*. a) Competitive suppression of the GlcNAz incorporation. The seedlings treated with 100  $\mu$ M Ac<sub>4</sub>GlcNAz alone, or together with 1 mM Ac<sub>4</sub>GlcNAc for 48 h, followed by fixation and click-labeling with alkyne–Alexa Fluor 488. Representative fluorescence images are shown in the left panel. Scale bar: 100  $\mu$ m. b) Statistical analysis of the fluorescence intensity of (a). The error bars represent the S.D. from more than 60 cells. Data of those cells were collected from six seedlings from three replicate experiments. \*\* $P < 0.01$  (Student's  $t$  test). c) Inhibition of GlcNAz incorporation by the N-glycosylation inhibitor. Seedlings were treated with 100  $\mu$ M Ac<sub>4</sub>GlcNAz for 48 h in the presence of 100 ng mL<sup>-1</sup> tunicamycin. Scale bars: 100  $\mu$ m. d) Statistical analysis of the fluorescence intensity of c). The error bars represent the S.D. from more than 60 cells. Data of those cells were collected from six seedlings from three replicate experiments. \*\* $P < 0.01$  (Student's  $t$  test). e) Western blot analysis of the GlcNAz-labeled and enriched glycoproteins. The Ac<sub>4</sub>GlcNAz- or DMSO-treated seedlings were lysed and reacted with 100  $\mu$ M alkyne–biotin via CuAAC, followed by enrichment with streptavidin beads. For releasing N-linked glycans, the beads were incubated with PNGase F for 24 h. The enriched proteins were then subjected to *anti*-biotin immunoblot analysis.

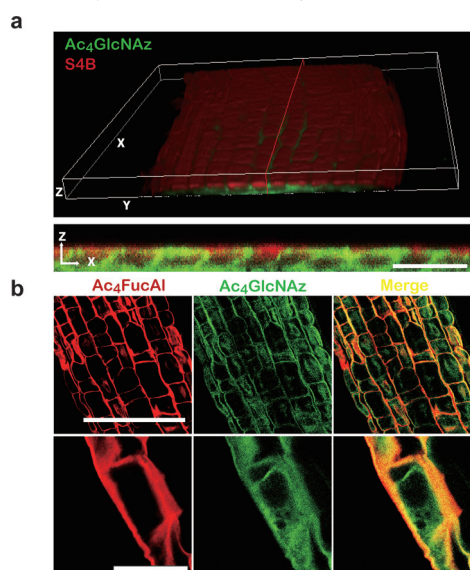


**Figure 4.** GlcNAz is incorporated into N-linked glycoproteins located both in the cell wall and on the plasma membrane. a) Colocalization between GlcNAz and S4B. The seedlings were treated with 100  $\mu$ M Ac<sub>4</sub>GlcNAz and click-labeled with alkyne–Alexa Fluor 488, followed by staining with 0.01 % S4B for 30 min. Top panel: two-color 3D reconstructed image of root epidermal cells. The frame size is 220  $\mu$ m  $\times$  220  $\mu$ m  $\times$  13.5  $\mu$ m. Bottom panel:  $x$ – $z$  projection from the position indicated by the red line in the top panel. Scale bar: 16  $\mu$ m. b) Colocalization between GlcNAz and FucAl. *Arabidopsis* seedlings were incubated with 100  $\mu$ M Ac<sub>4</sub>GlcNAz and 5  $\mu$ M Ac<sub>4</sub>FucAl for 72 h, followed by treatment with 0.8 M mannitol for 30 min. After fixation with PFA, the seedlings were sequentially reacted with azide–Cy5 and alkyne–Alexa Fluor 488. Scale bars: 100  $\mu$ m (top panel) and 20  $\mu$ m (bottom panel).

glycans during *Arabidopsis* development. In *Arabidopsis* roots, new cells produced by stem cells undergo three distinct developmental phases toward maturity, which defines the developmental zones of the root: division zone, elongation zone, and differentiation zone (Figure 5a).<sup>[39]</sup> Distribution of newly synthesized N-linked glycans in these developmental zones was visualized by confocal fluorescence microscopy in seedlings treated with Ac<sub>4</sub>GlcNAz for 48 h (Figure 5b). Distinct fluorescence intensities were observed in different developmental zones along the root tissue. Cells in the elongation zone lose the ability to divide, and instead expand rapidly in volume by increasing their length.<sup>[40]</sup> The fast cell elongation starts when cells leave the division zone and slows down when cells enter the differentiation zone.<sup>[41]</sup> Accordingly, we observed significantly lower intensity of GlcNAz labeling in the elongation zone, comparing to the division zone or the differentiation zone (Figure 5b). These results indicate that N-glycosylation may be regulated in a developmental stage-dependent manner.

In summary, we have developed a strategy for metabolic labeling and fluorescence imaging of N-linked glycans in *Arabidopsis* using the azido-

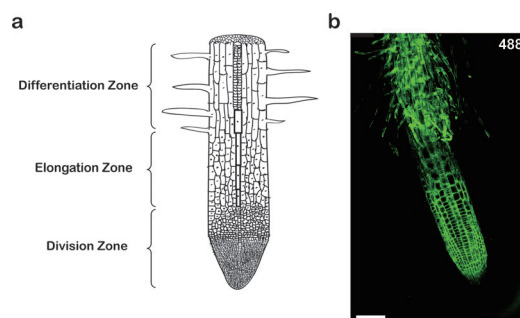


**Figure 5.** Distribution of newly synthesized N-glycans in the developmental zones of growing roots. a) Representation of distinct developmental zones of the *Arabidopsis* root: division zone, elongation zone, and differentiation zone. b) The seedlings were treated with 100  $\mu$ M Ac<sub>4</sub>GlcNAz for 48 h, followed by fixation and click-labeling. Confocal fluorescence images of a longitudinal section were collected through the root with a 63 $\times$  oil-immersion objective lens. The mosaic was then constructed from 12 titles (each 246  $\mu$ m  $\times$  246  $\mu$ m). Scale bar: 100  $\mu$ m.

sugar reporter, Ac<sub>4</sub>GlcNAz. Bioorthogonal conjugation of the incorporated azides with fluorescent probes allows direct visualization of the newly synthesized N-glycans in the root tissue. The presence of the GlcNAc salvage pathway in *Arabidopsis* is crucial to the success of metabolic labeling of N-glycans using GlcNAz. Our results add another piece of evidence to support the existence of GlcNAc salvage pathway. More importantly, our strategy provides a means to visualize the protein N-linked glycosylation in *Arabidopsis* seedlings with spatial and temporal resolution.

It is likely that UDP-GlcNAz can also be used as the sugar donor for O-GlcNAcylation and thus results in metabolic labeling of intracellular O-GlcNAcylated proteins. In this work, the membrane impermeability of the fluorescent probes was exploited to ensure specific imaging of N-linked glycans located outside the membrane. On the other hand, Ac<sub>4</sub>GlcNAz may potentially be exploited as a chemical reporter for O-GlcNAc. Although thousands of O-GlcNAc-modified proteins have been discovered in animals, only a handful of O-GlcNAcylated proteins have been identified in plants.<sup>[30–32]</sup> In this pursuit, it is valuable to develop methods based on metabolic glycan labeling to profile the O-GlcNAc-modified proteome.

## Acknowledgements

We thank Prof. H. Guo and Y. Zhu for the assistance on plant culture and growth experiments, Dr. W. Zhou in the mass spectrometry facility of the National Center for Protein Sciences at Peking University for assistance with proteomic analysis. This work is supported by the National Natural Science Foundation of China (No. 21425204).

**Keywords:** *Arabidopsis thaliana* · metabolic labeling · N-linked glycans · plant glycobiology · salvage pathway

**How to cite:** *Angew. Chem. Int. Ed.* **2016**, *55*, 9301–9305  
*Angew. Chem.* **2016**, *128*, 9447–9451

- [1] C. Somerville, S. Bauer, G. Brininstool, M. Facette, T. Hamann, J. Milne, E. Osborne, A. Paredez, S. Persson, T. Raab, et al., *Science* **2004**, *306*, 2206–2211.
- [2] D. J. Cosgrove, *Nat. Rev. Mol. Cell Biol.* **2005**, *6*, 850–861.
- [3] I. B. H. Wilson, *Curr. Opin. Struct. Biol.* **2002**, *12*, 569–577.
- [4] D. F. Zielinska, F. Gnad, K. Schropp, J. R. Wiśniewski, M. Mann, *Mol. Cell* **2012**, *46*, 542–548.
- [5] E. Nguema-Ona, M. Vicié-Gibouin, M. Gotté, B. Plancot, P. Lerouge, M. Bardor, A. Driouich, *Front. Plant Sci.* **2014**, *5*, 499.
- [6] A. Varki, R. D. Cummings, J. D. Esko, H. H. Freeze, G. W. Hart, M. E. Etzler, *Essentials of Glycobiology*, Cold Spring Harbor Laboratory Press, New York, **2008**.
- [7] S. T. Laughlin, C. R. Bertozzi, *Proc. Natl. Acad. Sci. USA* **2009**, *106*, 12–17.
- [8] M. Attreed, M. Desbois, T. H. van Kuppevelt, H. E. Bülow, *Nat. Methods* **2012**, *9*, 477–479.
- [9] E. L. Bird-Lieberman, A. A. Neves, P. Lao-Sirieix, M. O'Donovan, M. Novelli, L. B. Lovat, W. S. Eng, L. K. Mahal, K. M. Brindle, R. C. Fitzgerald, *Nat. Med.* **2012**, *18*, 315–321.
- [10] S. T. Laughlin, J. M. Baskin, S. L. Amacher, C. R. Bertozzi, *Science* **2008**, *320*, 664–667.
- [11] J. Rong, J. Han, L. Dong, Y. Tan, H. Yang, L. Feng, Q.-W. Wang, R. Meng, J. Zhao, S.-Q. Wang, et al., *J. Am. Chem. Soc.* **2014**, *136*, 17468–17476.
- [12] A. A. Neves, Y. A. Wainman, A. Wright, M. I. Kettunen, T. B. Rodrigues, S. McGuire, D.-E. Hu, F. Bulat, S. Geninatti Crich, H. Stöckmann, et al., *Angew. Chem. Int. Ed.* **2016**, *55*, 1286–1290; *Angew. Chem.* **2016**, *128*, 1308–1312.
- [13] M. Pauly, K. Keegstra, *Plant J.* **2008**, *54*, 559–568.
- [14] C. T. Anderson, I. S. Wallace, C. R. Somerville, *Proc. Natl. Acad. Sci. USA* **2012**, *109*, 1329–1334.
- [15] M. Sawa, T.-L. Hsu, T. Itoh, M. Sugiyama, S. R. Hanson, P. K. Vogt, C.-H. Wong, *Proc. Natl. Acad. Sci. USA* **2006**, *103*, 12371–12376.
- [16] M. Dumont, A. Lehner, B. Vauzeilles, J. Malassis, A. Marchant, K. Smyth, B. Linclau, A. Baron, J. Mas Pons, C. T. Anderson, et al., *Plant J.* **2016**, *85*, 437–447.
- [17] E. Weerapana, B. Imperiali, *Glycobiology* **2006**, *16*, 91R–101R.
- [18] P. Lerouge, M. Cabanes-Macheteau, C. Rayon, A. C. Fischette-Lainé, V. Gomord, L. Faye, *Plant Mol. Biol.* **1998**, *38*, 31–48.
- [19] R. Strasser, *Front. Plant Sci.* **2014**, *5*, 363.
- [20] H. Koiwa, F. Li, M. G. McCully, I. Mendoza, N. Koizumi, Y. Manabe, Y. Nakagawa, J. Zhu, A. Rus, J. M. Pardo, et al., *Plant Cell* **2003**, *15*, 2273–2284.
- [21] H. C. Hang, C. Yu, D. L. Kato, C. R. Bertozzi, *Proc. Natl. Acad. Sci. USA* **2003**, *100*, 14846–14851.
- [22] D. J. Vocadlo, H. C. Hang, E.-J. Kim, J. A. Hanover, C. R. Bertozzi, *Proc. Natl. Acad. Sci. USA* **2003**, *100*, 9116–9121.
- [23] M. Boyce, I. S. Carrico, A. S. Ganguli, S.-H. Yu, M. J. Hangauer, S. C. Hubbard, J. J. Kohler, C. R. Bertozzi, *Proc. Natl. Acad. Sci. USA* **2011**, *108*, 3141–3146.
- [24] B. W. Zaro, Y.-Y. Yang, H. C. Hang, M. R. Pratt, *Proc. Natl. Acad. Sci. USA* **2011**, *108*, 8146–8151.
- [25] K. N. Chuh, B. W. Zaro, F. Piller, V. Piller, M. R. Pratt, *J. Am. Chem. Soc.* **2014**, *136*, 12283–12295.
- [26] C. M. Woo, A. T. Iavarone, D. R. Spiciarich, K. K. Palaniappan, C. R. Bertozzi, *Nat. Methods* **2015**, *12*, 561–567.
- [27] G. W. Hart, M. P. Housley, C. Slawson, *Nature* **2007**, *446*, 1017–1022.
- [28] E. P. Bennett, U. Mandel, H. Clausen, T. A. Gerken, T. A. Fritz, L. A. Tabak, *Glycobiology* **2012**, *22*, 736–756.
- [29] M. Bar-Peled, M. A. O'Neill, *Annu. Rev. Plant Biol.* **2011**, *62*, 127–155.
- [30] N. E. Olszewski, C. M. West, S. O. Sassi, L. M. Hartweck, *Biochim. Biophys. Acta Gen. Subj.* **2010**, *1800*, 49–56.
- [31] E. Steiner, I. Efroni, M. Gopalraj, K. Saathoff, T.-S. Tseng, M. Kieffer, Y. Eshed, N. Olszewski, D. Weiss, *Plant Cell* **2012**, *24*, 96–108.
- [32] R. Zentella, J. Hu, W.-P. Hsieh, P. A. Matsumoto, A. Dawdy, B. Barnhill, H. Oldenhof, L. M. Hartweck, S. Maitra, S. G. Thomas, et al., *Genes Dev.* **2016**, *30*, 164–176.
- [33] M. Nozaki, M. Sugiyama, J. Duan, H. Uematsu, T. Genda, Y. Sato, *Plant Cell* **2012**, *24*, 3366–3379.
- [34] K. Furo, M. Nozaki, H. Murashige, Y. Sato, *FEBS Lett.* **2015**, *589*, 3258–3262.
- [35] F. Altmann, S. Schweiszer, C. Weber, *Glycoconjugate J.* **1995**, *12*, 84–93.
- [36] W. Song, R. A. Mentink, M. G. L. Henquet, J. H. G. Cordewener, A. D. J. van Dijk, D. Bosch, A. H. P. America, A. R. van der Krol, *J. Proteomics* **2013**, *93*, 343–355.
- [37] S.-L. Xu, K. F. Medzihradsky, Z.-Y. Wang, A. L. Burlingame, R. J. Chalkley, *Mol. Cell. Proteomics* **2016**, DOI: 10.1074/mcp.M115.056101.
- [38] C. T. Anderson, A. Carroll, L. Akhmetova, C. Somerville, *Plant Physiol.* **2010**, *152*, 787–796.
- [39] J. J. Petricka, C. M. Winter, P. N. Benfey, *Annu. Rev. Plant Biol.* **2012**, *63*, 563–590.
- [40] J.-P. Verbelen, T. De Cnodder, J. Le, K. Vissenberg, F. Baluska, *Plant Signaling Behav.* **2006**, *1*, 296–304.
- [41] J. Le, F. Vandenbussche, D. Van Der Straeten, J. P. Verbelen, *Physiol. Plant.* **2004**, *121*, 513–519.

Received: March 28, 2016

Revised: May 20, 2016

Published online: June 27, 2016